

EUROPEAN COOPERATION
IN THE FIELD OF SCIENTIFIC
AND TECHNICAL RESEARCH

COST 273 TD(03)061
Barcelona, Spain
January 15-17, 2003

EURO-COST

SOURCE: *ftw.* Forschungszentrum Telekommunikation
Wien

Information and Communication Mobile
Siemens AG

Telenor R&D

**Spatial and temporal long term properties of typical urban base stations at
different heights**

H. Hofstetter, I. Viering, P. H. Lehne

ftw. Forschungszentrum Telekommunikation Wien
Donau City Strasse 1
A-1220 Vienna
Austria
Phone: +43 1 505 2830 25
Fax: +43 1 505 2830 99
Email: hofstetter@ftw.at

Spatial and temporal long term properties of typical urban base stations at different heights

Helmut Hofstetter¹⁾, Ingo Viering²⁾, Per H. Lehne³⁾

¹⁾Forschungszentrum Telekommunikation Wien, Donau-City-Straße 1, 1220 Vienna, Austria.

²⁾Siemens AG, Lise-Meitner-Straße 13, 89081 Ulm, Germany.

³⁾Telenor R&D N-1331 Fornebu, Norway.

hofstetter@ftw.at

Abstract

This paper presents first results of a MIMO measurement campaign which has taken place in Oslo during summer 2002. The main focus of the paper is on the spatial long term properties of the radio channel in dense urban areas. Two different base station antenna heights at the same area are investigated, one antenna position at rooftop level and one at street level. The F-eigen-ratio is used for the quantification of the long term effects and the eigenvalue distributions are given. The results are compared with former measurements conducted in Vienna.

1 Introduction

Almost all beamforming methods proposed for mobile communication systems [2] are based on the assumption, that the spatial properties of the channel change very slowly. This is strongly related to the wide sense stationarity assumption [3] which says that second order statistics can be viewed constant over certain time intervals.

Whereas a lot of algorithms apply this assumption inherently, [4] explicitly distinguishes between short-term and long-term properties. The first account for the changing interference situation ("fast fading", small-scale effects) and the latter expresses the current environment in terms of delays, doppler frequencies, direction of arrival/departure, average power ("slow-fading", large-scale effects) [5].

The spatial properties are often considered as spatial covariance matrices [6].

This paper is based on measurement data from a measurement campaign carried out in summer 2002 by the FLOWS consortium [1] in Oslo. Two dense urban area scenarios were chosen trying to quantify the long term effects by usage of a newly introduced measure, the F-eigen-ratio [7]. The paper is structured in the following way: Section 2 gives a detailed overview on the used measurement equipment followed by a description of the chosen environment (Section 3). The F-eigen-ratio is briefly reviewed in Section 4. Results are shown in Section 5 and Section 6 concludes the paper.

2 Measurement equipment

The equipment used for the measurements is a wideband channel sounder with synchronized switching between transmitter and receiver. It was manufactured by SINTEF Telecom and Informatics in Trondheim, Norway, on assignment from Telenor R&D in 2001. It consists of one transmitter part (Figure 1) and one receiver part (Figure 2) that can be placed arbitrarily apart from each other. The sounder was operated at a center frequency of 2.1GHz and a

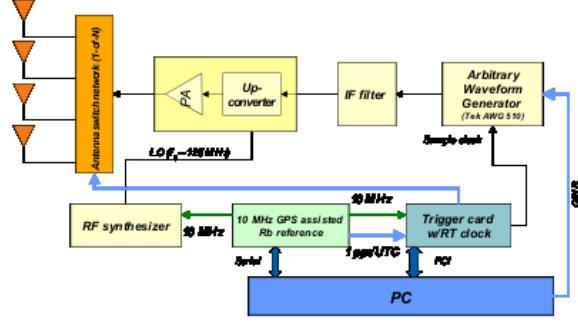


Figure 1: Block diagram of transmitter.

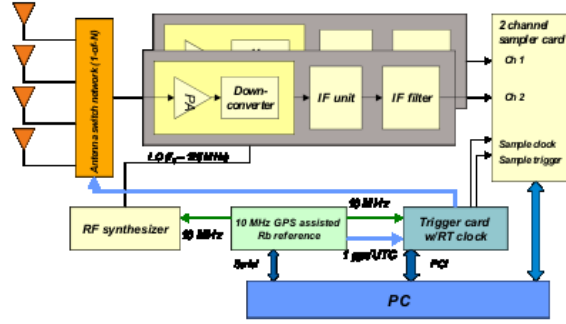


Figure 2: Block diagram of receiver.



Figure 3: Measurement setup at transmitter.

bandwidth of 50MHz was chosen. The measurement period, which is the time between two MIMO measurements, was set to 200ms. The Tx-trolley was moved at speeds of about 1kmh resulting in a snapshot resolution in space of about Lambda halve. The measurement setup is given in Figure 3.

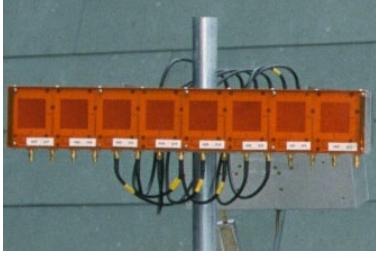


Figure 4: Tx antenna.

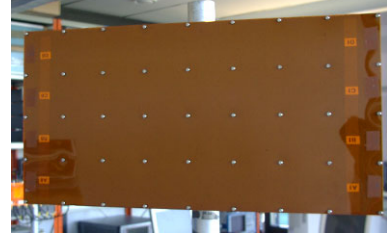


Figure 5: Rx antenna.

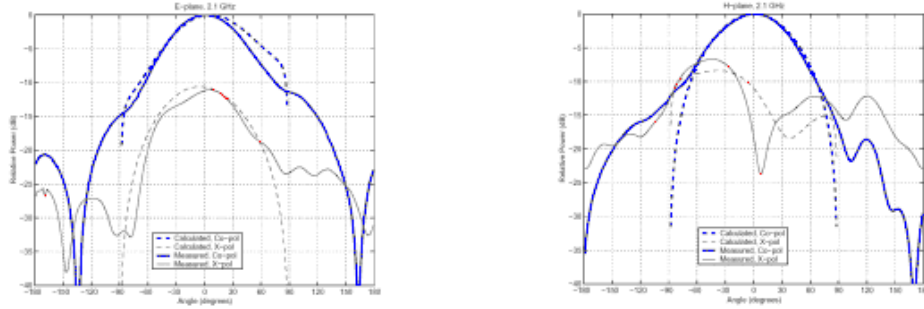


Figure 6: Diagram of one antenna element. Left: E-plane. Right: H-plane.

2.1 Antennas and switching

Both transmitter and receiver antennas are broadband, dual polarized patch arrays with integrated switching networks. The transmitter antenna (Figure 4) is an 8 element uniform linear array (ULA). The center frequency is 2.1 GHz and each element has a bandwidth (VSWR < 2.0) of 330 MHz [11]. Each element is a rectangular patch and has two ports, one for each polarization. The 3 dB beamwidth is approx 60° . Typical element diagrams (E- and H-plane) are shown in Figure 6. The diagrams also show the cross polar discrimination.

The element spacing is 71.4 mm corresponding to $\lambda/2$ at 2.1 GHz. Because each element has two ports, the array in total has 16 ports which can be connected arbitrarily to a 1-of-8 switching network. In the measurements performed, the 4 center elements were used with both ports connected. In this way, the effects of polarization on MIMO performance were investigated. The specification for the switches made it necessary to limit transmitter output power to 0.5 W (27 dBm).

The receiver antenna follows the same concept, but this is a planar array, i.e. two-dimensional with 8 elements horizontally and 4 vertically, giving a total of 32 elements 5. The elements were identical to the transmitter case, however the element spacing is slightly different: 73 mm (0.51λ). The individual ports of the antenna elements were not available on this antenna. A duplicated switching network was integrated giving access to the switched signal from both polarizations. This meant that only one polarization could be measured at a time. For the measurements, only vertical polarization was investigated. The receiver antenna used all elements and was switched row-wise.

3 Measurement scenario

The measurement site is in a part of Oslo with a regular street grid. The building mass is homogenous and materials used are mostly brick and concrete. The building height varies from



Figure 7: Measurement scenario.



Figure 8: Map of the measurement area and measured tracks (red).

20-30 m. The area is often referred to as 'Kvadraturen'.

The site fits well with some of the COST259 [12] micro cellular scenarios (GTU, GBU, GSN, GSC, GSX). Measurements at this site were taken twice, once with the receiver antenna on street level (Rx1) and once with the antenna on rooftop level on top of a hotel building (Rx2). Thus, these two antenna positions will cover typical micro- and pico-cellular base station scenarios. Some impressions of the area are given in Figure 7. The measurement routes used are shown on the map in Figure 8.

4 F-eigen-ratio

In [7] the *F-eigen-ratio* is already introduced. It is a measure describing the discrepancy between two covariances. The name emphasizes the fact, that the eigen structure of the matrices is considered [4].

Translated to the spatial long-term variations, a spatial covariance matrix $\mathbf{R}(t_0 - \Delta t)$ is measured at time $t_0 - \Delta t$ and applied at time t_0 , where the spatial structure might have changed described by a covariance matrix $\mathbf{R}(t_0)$. The F-eigen-ratio accounts for the resulting SNR loss. In the following the F-eigen-ratio definition is briefly recalled. The considered covariance matrices are members of the complex space $\mathcal{C}^{K_a \times K_a}$ where K_a is the number of antennas. At first

the eigenvalue decompositions

$$\mathbf{R}(t_0 - \Delta t) = \hat{\mathbf{W}} \cdot \hat{\mathbf{\Lambda}} \cdot \hat{\mathbf{W}}^H \quad ; \quad \mathbf{R}(t_0) = \mathbf{W} \cdot \mathbf{\Lambda} \cdot \mathbf{W}^H \quad (1)$$

are computed where $\hat{\mathbf{\Lambda}}, \mathbf{\Lambda} \in \mathcal{R}^{K_a \times K_a}$ are diagonals with the eigenvalues of $\mathbf{R}(t_0 - \Delta t), \mathbf{R}(t_0)$ as entries, and the columns of $\hat{\mathbf{W}}, \mathbf{W} \in \mathcal{C}^{K_a \times K_a}$ are the corresponding eigenvectors. The hat stresses the outdated nature of the eigenvectors $\hat{\mathbf{W}}$ and eigenvalues $\hat{\mathbf{\Lambda}}$, whereas \mathbf{W} and $\mathbf{\Lambda}$ are the correct values, which are assumed to be unavailable.

Furthermore, the reduced versions $\hat{\mathbf{W}}_F, \mathbf{W}_F \in \mathcal{C}^{K_a \times F}$ of the matrices $\hat{\mathbf{W}}, \mathbf{W}$ are introduced, which contain the eigenvectors corresponding to the F largest eigenvalues of the covariance matrices $\mathbf{R}(t_0 - \Delta t)$ and $\mathbf{R}(t_0)$, respectively. Then, the F-eigen-ratio is defined as

$$q_{\text{eigen}}^{(F)}(\Delta t) = \frac{\text{tr} \left\{ \hat{\mathbf{W}}_F^H \cdot \mathbf{R}(t_0) \cdot \hat{\mathbf{W}}_F \right\}}{\text{tr} \left\{ \mathbf{W}_F^H \cdot \mathbf{R}(t_0) \cdot \mathbf{W}_F \right\}} \quad (2)$$

with the properties $0 \leq q_{\text{eigen}}^{(F)}(\Delta t) \leq 1$, $q_{\text{eigen}}^{(F=K_a)}(\Delta t) = 1 \forall \Delta t$ and $q_{\text{eigen}}^{(F)}(0) = 1 \forall F$.

In other words, the F-eigen-ratio expresses the loss due to the application of outdated antenna weights $\hat{\mathbf{W}}_F$ instead of the correct weights \mathbf{W}_F .

In the line-of-sight case, $q_{\text{eigen}}^{(F=1)}$ matches beam pattern values, where the azimuth axis is transformed to Δt values. This is demonstrated in [8] for one LOS scenario.

With larger F -values, $q_{\text{eigen}}^{(F)}$ typically decreases, since it is more likely to hit energy carrying dimensions in the current signal space with the outdated weight vectors $\hat{\mathbf{W}}_F$. However, the columns in $\hat{\mathbf{W}}_F$ do not decorrelate the channel, i.e. the off-diagonal values of $\hat{\mathbf{W}}_F^H \cdot \mathbf{R}(t_0) \cdot \hat{\mathbf{W}}_F$ are non-zero. This effect is not captured by the F-eigen-ratio.

5 Results

From all measurements spatial covariance matrices were extracted as described in [7], which will be reviewed in the sequel.

5.1 Extraction of the Covariance Matrices

From the measured impulse responses a 5MHz band was used only, which is a typical bandwidth for 3rd generation mobile communication [10]. For all investigations in this paper only one row (8 elements) of the receive antenna elements was used. The spatial covariance matrix was set up by incoherently averaging over all delay values, all transmit antennas and a time interval Δt_{avg} . A covariance matrix was initiated each Δt_{new} seconds.

Special attention was paid to the choice of the parameters Δt_{avg} . On one hand, it should be large enough so that all short-term effects are eliminated by averaging. Otherwise, the rank of the matrices would decrease. On the other hand, a too large value would violate the WSS assumption already within a single covariance pretending a higher rank than the true one.

The chosen values of $\Delta t_{avg} = 6\text{sec}$ resulted in relatively smooth F-eigen-ratio curves over time. This suggests that the averaging was long enough to achieve stable matrices. On the other hand the rank of the matrices is even smaller than expected, so that the choice of Δt_{avg} seems to be reasonable.

The parameter Δt_{new} was set to a slightly smaller value than Δt_{avg} to establish a small temporal overlapping between the matrices. The values of Δt for the following investigations are multiples of Δt_{new} .

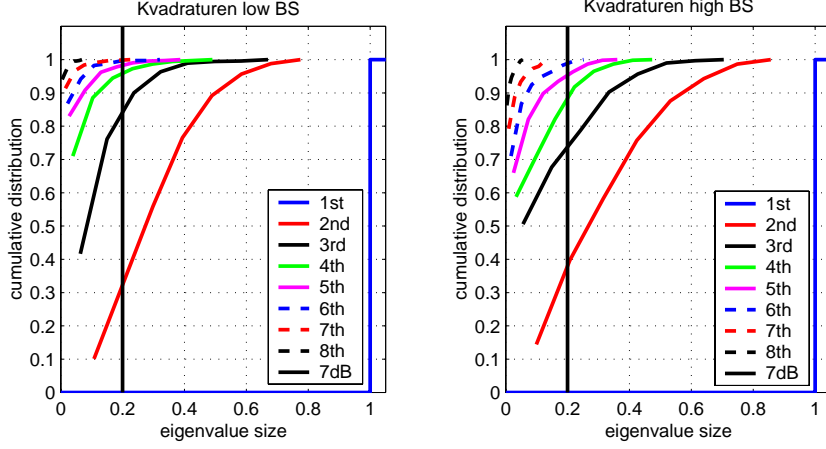


Figure 9: Eigenvalue distribution.

5.2 Eigenvalue distributions

Figure 9 shows the cdf of the eigenvalue distribution of all measured covariance matrices for both antenna positions. Note that the strongest eigenvalue is always normalized to one. In contrast to the Vienna measurements [9], with even a higher base station position, the channel is more dispersive. Compared to the Vienna measurements [9] there is about one additional eigenvalue with significant power visible.

5.3 F-eigen-ratio

For a certain value of Δt all occurring pairs $\{\mathbf{R}(t_0 - \Delta t); \mathbf{R}(t_0)\}$ are considered. For each pair, the F-eigen-ratio $q_{eigen}^{(F)}(\Delta t)$ was evaluated using $F = 1$. Each curve in the Figures 10 depicts the cumulative distribution function (CDF) of the F-eigen-ratio $q_{eigen}^{(F)}(\Delta t)$ for a single value of Δt .

In addition to the F-eigen-ratio the *long-term time constant* τ_{LT} is defined like in [9]:

Definition: The spatial long-term time constant τ_{LT} is the time difference Δt for which the $(F = 1)$ -eigen-ratio $q_{eigen}^{(F=1)}(\Delta t)$ is less than 1dB in 90% of all cases.

This time constant corresponds to the CDF curve crossing the point (1dB; 90%). Other definitions of the long-term time constant would change the following results quantitatively, but not qualitatively.

5.4 Wide Sense Stationarity

First we try to assess, to what extend the WSS assumption is fulfilled for our setup. To this end, we compare the long-term time constant τ_{LT} derived in the previous section with the coherence time of the channel τ_{coh} .

The most common definition of the coherence time is the duration of one cycle of the maximum doppler frequency. The velocity of the mobile was about 1kmh translating to a doppler frequency of 2Hz for a carrier frequency of 2.1GHz. The coherence time is the reciprocal of the doppler frequency, i.e. 500ms.

To get a measure for the spatial WSS quality Q_{WSS} a quotient

$$Q_{WSS} = \frac{\tau_{LT}}{\tau_{coh}} \quad (3)$$

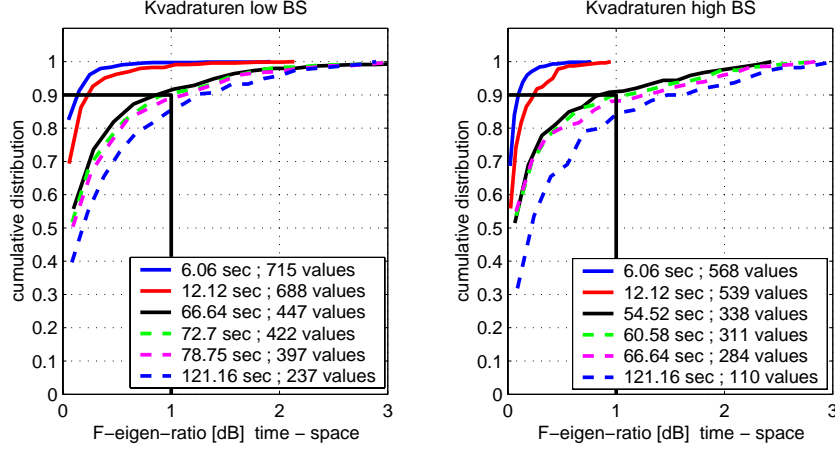


Figure 10: F-eigen-ratio.

is defined as described in [9] which is a number expressing how many multiples of the coherence time the spatial properties can be considered constant.

Table 1 summarizes the results for the WSS quality and compares them to a measurement

environment	low BS	high BS	Vienna
long-term time constant τ_{LT}	73sec	61sec	22.6sec
coherence time τ_{coh}	500ms	500ms	180ms
WSS Quality Q_{WSS}	146	122	126

Table 1: Long-term Time constant, Coherence Time and WSS Quality

taken in Vienna [9]. Again, the WSS quality is in the range of 100 which seems to be a typical value for outdoor environments.

5.5 Receive power level

Figure 11 shows the receive power level for one measurement run for both antenna heights. The measurement is a NLOS case (Figure 12) starting at the corner closer to the receiver with the Tx antenna pointing away from the movement. The most important propagation effect is wave guiding through streets. First, the receive power level for the high base station position is about 5 to 10dB lower than for the position at street level which is mostly due to the antenna characteristic at the base station. For higher elevation angles the patch array is less sensitive.

From a channel modelling point of view the occurrence of additional scatterer clusters for a very limited time stays in contrast to the COST 259 micro cellular model with relatively huge visibility regions. Especially for the high BS position some additional clusters are only visible for a range of about 5 to 10m. These additional clusters push the power level by about 5dB. Further investigations will be necessary to understand this effect.

Another effect which is visible in the beginning of the measurement run is the diffraction over the edge of the house in the corner leading to slightly higher power levels for the low base station position.

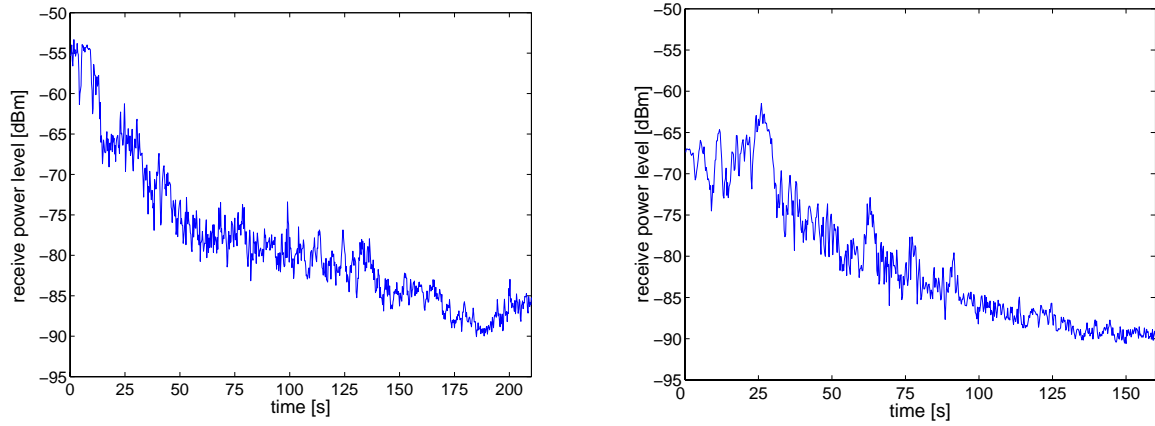


Figure 11: Receive power level. Left: low BS. Right: high BS.

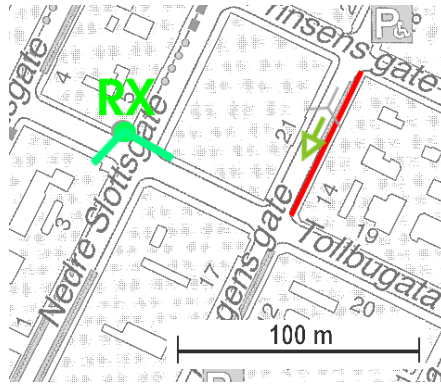


Figure 12: Measurement run.

6 Conclusion

Initial evaluations of a wideband MIMO measurement campaign carried out in Oslo were presented. The focus of this document is on the description of the measurement setup and the used channel sounder.

The results show some similarities with the Vienna measurements but the scenario is more dispersive which may be due to the lower BS positions.

In contrast to the COST 259 channel model additional clusters could be identified which are only visible for very limited areas.

The FLOWS consortium has spent a lot of effort on measuring the MIMO channel in the 2GHz band and measurements at 5GHz will follow in the near future.

7 Acknowledgement

The authors would like to thank Wolfgang Utschick for various helpful discussions and Magne Pettersen for his support during the measurement campaigns.

This work is being performed in the framework of the IST project FLOWS IST-2001-32125 which is partially funded by the European Union. The authors would like to acknowledge the contribution to this work by their colleagues in their respect companies.

References

- [1] FLOWS Project Home Page, *Flexible Convergence of Wireless Standards and Services*, www.flows-ist.org.
- [2] L. C. Godara, "Application of Antenna Arrays to Mobile Communications, Part II: Beam-Forming and Direction-of-Arrival Considerations," *Proceedings of the IEEE*, Vol 85 No. 8, August 1997.
- [3] P. A. Bello, "Characterization of Randomly Time-Variant Linear Channels," *IEEE Transactions on Communications Systems*, vol. 11, pp. 360-393, 1963.
- [4] C. Brunner, W. Utschick, J.A. Nossek, "Exploiting the short-term and long-term channel properties in space and time: eigenbeamforming concepts for the BS in WCDMA," *European Transactions on Telecommunications, Special Issue on Smart Antennas*, VOL. 5, 2001.
- [5] R.B. Ertel, P. Cardieri, K.W. Sowerby, T.S. Rappaport, J.H. Reed, "Overview of spatial channel models for antenna array communication systems," *IEEE Personal Communications*, Vol. 5, No. 1, pp. 10-22, February 1998.
- [6] J. Salz, J. H. Winters, "Effect of Fading Correlation on Adaptive Arrays in Digital Wireless Communications," *IEEE International Conference on Communications ICC'93*, Geneva, Switzerland, pp. 1768-1774, 1993.
- [7] I. Viering, H. Hofstetter, W. Utschick, "Validity of Spatial Covariance Matrices over Time and Frequency," *IEEE Globecom 02*, Taipei, Taiwan, November 2002.
- [8] H. Hofstetter, I. Viering, W. Utschick, "Evaluation of Suburban measurements by eigenvalue statistics," *COST273 1st Workshop*, Espoo, Finland, May 2002.
- [9] I. Viering, H. Hofstetter, W. Utschick, "Spatial Long-Term Variations in Urban, Rural and Indoor Environments," *TD-02-135 COST273 5th Meeting*, Lisbon, Portugal, Sept. 2002.
- [10] Specification Home Page, *3rd Generation Partnership Project*, www.3gpp.org/specs/specs.htm.
- [11] Skyttemyr, S.A., Hansen, P.S., Alsos, O. "A Broadband Cavity-backed Microstrip Antenna with Dual Linear Polarisation and Direct Microstrip Line Feeding". *AP2000 Millennium Conference on Antennas & Propagation*, Davos, Switzerland, April 2000.
- [12] L. M. Correia (Editor), *WIRELESS FLEXIBLE PERSONALIZED COMMUNICATIONS, final report of COST Action 259*, Wiley, 2001.